Available online at www.sciencedirect.com
SCIENCE DIRECT®
Journal of Photochemistry and Photobiology A: Chemistry 160 (2003) 55–60
Journal of Photochemistry and Photobiology A:Chemistry
www.elsevier.com/locate/jphotochem

Effects of surface fluorination of TiO_2 on the photocatalytic degradation of tetramethylammonium

Muhammad Shariq Vohra, Soonhyun Kim, Wonyong Choi*

School of Environmental Science and Engineering, Pohang University of Science and Technology, Pohang 790-784, South Korea

Received 19 December 2002; received in revised form 28 January 2003; accepted 10 April 2003

Abstract

Photocatalytic degradation (PCD) of tetramethylammonium (TMA, $(CH_3)_4N^+$) ions in water was studied using both naked-TiO_2 and fluorinated-TiO_2 (F–TiO_2) in order to investigate how the modification in TiO_2 surface functional groups affects the PCD reaction. A comparison between the naked-TiO_2 and F–TiO_2 systems shows that their relative photoreactivities strongly depend on pH. At pH 3, the addition of fluoride decreases the PCD rate whereas higher degradation rates are obtained at pH 5 and 7 with F–TiO_2. Little fluoride effect on the TMA degradation rate is observed at pH 9. The addition of fluoride affects not only the PCD rate but also the mechanistic pathways of TMA degradation and subsequently the intermediates and product distribution. The modeling result of TiO_2 surface speciation shows that the fluoride addition at pH 3 shifts the dominant surface species from Ti–OH_2^+ and Ti–OH to Ti–F (to near completion). This reduces the surface positive charge of TiO_2 (at pH 3) upon adding fluoride and consequently lowers the electrostatic repulsion between the TMA cations and TiO_2 surface. Accordingly, ATR-FTIR spectroscopic measurements show that the TMA concentration at the water/TiO_2 interface is higher on F–TiO_2 than naked-TiO_2 film at pH 3. However, the PCD of TMA on F–TiO_2 at pH 3 is reduced on the contrary, which is ascribed to the depletion of surface OH groups that are the site of surface OH radical formation. At pH 5 and 7, the surface OH sites are not completely diminished even in the presence of fluoride and the presence of surface Ti–F species in fact increases the TMA degradation rate. The fluoride-induced enhancement of PCD is yet to be understood although some speculative arguments are presented.

Keywords: TiO_2; Photocatalytic degradation; Tetramethylammonium; Fluoride; Surface speciation

1. Introduction

TiO_2 photocatalysis that is based upon photo-induced interfacial charge transfer processes has been intensively studied for its application to the destruction of toxic pollutants [1–7]. Several studies have reported the significance of TiO_2 surface speciation in the photocatalytic degradation (PCD) processes [8–12]. Speciation of the TiO_2 surface groups and substrates (with acidic or basic functional groups) is pH-dependent and thus significantly alters the PCD trend with changing pH. For anionic species, higher adsorption (through electrostatic attractions) and faster degradation result at lower pH ($<pH_{zpc}$), whereas cationic substrates show increased adsorption and degradation at higher pH ($>pH_{zpc}$) [11]. Modifications in TiO_2 surface properties have been also reported to increase both surface adsorption and degradation of aquatic contaminants [13–15].

The adsorption of fluoride on TiO_2 surface is known to replace the surface hydroxyl groups with Ti–F species and significantly changes the photocatalytic reactivity of TiO_2. Minero et al. [16,17] studied the PCD of phenol using fluorinated-TiO_2 (F–TiO_2) and observed that the degradation rates of phenol and its intermediates (hydroquinone and catechol) were much enhanced with F–TiO_2. They claimed that the enhancement effect was mainly related to the reaction of homogenous free OH radicals whose formation was favored on F–TiO_2. On the other hand, the adsorption of other inorganic anions on TiO_2 has been also reported to alter the PCD rate [18,19].

The present study investigated the PCD of tetramethylammonium (TMA, $(CH_3)_4N^+$) employing naked-TiO_2 and F–TiO_2. TMA represents a unique case of recalcitrant organic cations whose surface interaction on TiO_2 surface is mostly electrostatic and whose chance of direct electron transfer reactions on TiO_2 is insignificant. Since the PCD of TMA on TiO_2 is initiated by the photogenerated OH radicals [7], it should serve as a good model compound when the relationship between the surface speciation and OH radical mediated reactions is investigated. The effects of fluoride on TMA PCD were investigated under different experimental conditions. The resulting differences in

* Corresponding author. Tel.: +82-54-279-2283; fax: +82-54-279-8299.
E-mail address: wchoi@postech.ac.kr (W. Choi).

1010-6030/03/$ – see front matter © 2003 Elsevier Science B.V. All rights reserved.
doi:10.1016/S1010-6030(03)00221-1

PCD trends are related to the pertinent changes in the TiO_2 surface speciation.

2. Experimental

2.1. Reagents and materials

The following reagent-grade chemicals were used as received: TiO_2 (Degussa P25), $(CH_3)_4NCl$ (ACROS Organics), $(CH_3)_3NHCl$ (Aldrich), $(CH_3)_2NH_2Cl$ (Sigma), $(CH_3)NH_3Cl$ (Sigma), NH_4Cl (Aldrich), NaF (Samchun Chemicals, Korea), *tert*-butyl alcohol (S.P.C. GR Reagent, Japan), NaCl (S.P.C. GR Reagent, Japan), methanesulfonic acid (Aldrich), $NaCO_3$ (S.P.C. GR Reagent, Japan), $NaHCO_3$ (Kanto, Japan), HCl (S.P.C. GR Reagent, Japan), $HClO_4$ (Aldrich), and NaOH (S.P.C. GR Reagent, Japan). A Barnstead water purification setup was employed to obtain the deionized water (18 MΩ cm).

2.2. Photocatalysis

All PCD experiments were carried out using a Pyrex reactor (33 ml) with a quartz window. The TiO_2 particles (at 0.5 g/l) were first well suspended in 27 ml deionized water by sonicating for 30 s. For the experiments using the F–TiO_2, NaF was added to the aqueous suspension to obtain the F–TiO_2 suspension. An aliquot of 3 ml from 1 mM TMA stock solution was then added to obtain an initial $[(CH_3)_4N^+]_0 = 100\,\mu M$. The pH of the suspension was adjusted with HCl or NaOH standard solutions. An Xe-arc lamp (300 or 450 W, Oriel) with a 10 cm IR water filter and a UV-cutoff ($\lambda > 300$ nm) filter was used as the illumination source. Sample aliquots of 1 ml were collected at appropriate time intervals and filtered through 0.45 μm PTFE filters (Millipore). The reactor was kept sealed using a rubber septum throughout the illumination period.

2.3. Analysis

The TMA and reaction products/intermediates were analyzed using a Dionex ion chromatograph (IC, DX-120) that was equipped with a conductivity detector, Dionex Ionpac CS-14 (4 mm × 250 mm; CG-14 Guard, 4 mm × 50 mm) for cation analysis and AS-14 (4 mm × 250 mm; AG-14 Guard, 4 mm × 50 mm) for anion analysis. The eluent compositions were 10 mM methanesulfonic acid for the cation analysis, and 3.5 mM Na_2CO_3/1 mM $NaHCO_3$ for the anion analysis. Fluoride (for fluoride adsorption experiment) was also analyzed using the IC setup.

The surface interactions of TMA cations with naked-TiO_2 and F–TiO_2 surface were investigated by monitoring their surface concentrations at the TiO_2 (or F–TiO_2)/water interface with using attenuated total reflection Fourier transform infrared spectroscopy (ATR-FTIR) [7]. Spectra were recorded using a FTIR spectrometer (Bomem, MB 104) equipped with a deuterated triglycine sulfate detector (DTGS) and an ATR unit (SpectraTech, ARK kit) with a horizontal ZnSe crystal. The ZnSe crystal (73 mm × 8 mm × 3 mm, crystal angle 45°) was bonded in a trough-shaped plate to hold liquid samples. The incident IR beam propagated within the crystal with 12 internal reflections. For the preparation of TiO_2 coating layer, 300 μl of suspension containing 0.76 mg of TiO_2 was applied over the one side of the ZnSe crystal plate and allowed to dry under ambient air. The TMA solution with or without fluoride was applied on the trough-plate and equilibrated with the TiO_2-coated ZnSe plate. The IR spectra of the TMA on the TiO_2/water interface were taken with varying the solution pH.

2.4. Modeling

The modeling of TiO_2 surface speciation was done employing the MINTEQA2/PRODEFA2 software equipped with the diffuse layer model [20]. Various surface properties of Degussa P25 TiO_2 as required for the surface speciation modeling have been reported earlier [21–23].

3. Results and discussion

Fig. 1 shows the initial PCD rates of TMA as a function of pH when naked-TiO_2 and F–TiO_2 were used. A comparison between the two catalyst systems shows a marked difference in their pH-dependent photoreactivity. For the naked-TiO_2, a V-shaped PCD trend is noted with higher degradation rates observed at pH 3 and 9 and lower at pH 5 and 7. This agrees with a recent observation made for the PCD of TMA using TiO_2 [7]. On the other hand, the PCD with F–TiO_2 is drastically reduced at pH 3 as compared to naked-TiO_2 but enhanced at higher pH. The photoreactivity of F–TiO_2 at pH 3 shows a gradual decrease in PCD

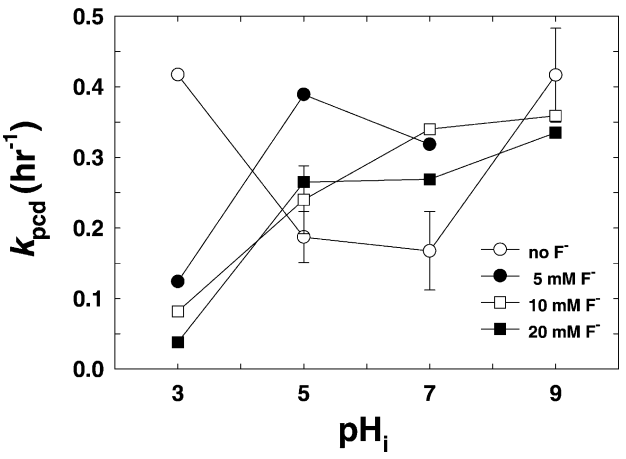

Fig. 1. TMA PCD rate constants (k_{pcd}: during the initial 2 h) as a function of the initial pH and fluoride concentration. $[TMA]_0 = 100\,\mu M$, $[TiO_2] = 0.5$ g/l.

Table 1
Concentrations (μM) of TMA and its degradation intermediates and products after 6 h PCD reactions[a] as a function of pH and fluoride concentration

[F⁻] (mM)	pH 3				pH 5				pH 7				pH 9		
	0	5	10	20	0	5	10	20	0	5	10	20	0	10	20
$[(CH_3)_4N^+]$	0	43	52	83	28	7	16	13	40	14	6	21	13	11	31
$[(CH_3)_3NH^+]$	20	27	21	3	10	15	21	24	0	0	0	0	2	0	0
$[(CH_3)_2NH_2^+]$	7	11	3	16	33	34	24	42	18	14	21	37	14	8	35
$[(CH_3)NH_3^+]$	9	0	0	0	7	15	20	18	12	13	15	40	9	11	35
$[NH_4^+]$	38	26	0	0	4	29	21	0	8	22	39	0	8	42	0
Total nitrogen	74	107	76	102	82	100	102	97	78	63	81	98	46	72	101

[a] $[TMA]_0 = 100\,\mu M$, $[TiO_2] = 0.5$ g/l (the same PCD reactions as those of Fig. 1).

rates with increasing $[F^-]$ up to 20 mM. The pH-dependent photocatalytic reactivities for TMA degradation can be divided into three distinct regions: (1) naked-TiO_2 > F–TiO_2 at around pH 3; (2) naked-TiO_2 < F–TiO_2 at pH 5–7; (3) naked-TiO_2 ≈ F–TiO_2 at around pH 9 (Fig. 1). However, in a previous study using F–TiO_2 the PCD rate of phenol was only enhanced with fluoride addition in the pH range 2–6 [16].

Table 1 summarizes the pH-dependent distribution of the major intermediates and products that were generated after 6 h PCD of TMA in the suspensions of naked-TiO_2 and F–TiO_2. They include $(CH_3)_3NH^+$, $(CH_3)_2NH_2^+$, $(CH_3)NH_3^+$, and NH_4^+ as also reported by Kim and Choi [7] and their concentrations strongly depend on the pH and $[F^-]$. Other products missing from Table 1 are nitrite and nitrate, which should explain for the N-mass deficits. The PCD of TMA has been previously proposed to proceed through successive demethylation steps to eventually generate NH_4^+ at acidic conditions or NO_2^-/NO_3^- at alkaline conditions where the neutral amine species are dominant [7]. However, in the present study, negligible TMA mineralization (i.e., NH_4^+ formation) is noted at all pH with 20 mM fluoride (Fig. 2). The presence of excess fluoride seems to inhibit complete mineralization to ammonium ions somehow though the demethylation of TMA does take place under all relevant conditions. On the other hand, the ammonium production is maximized when an optimal amount of fluoride is present in the range of pH 5–9 (Table 1). Negligible $(CH_3)_3NH^+$ formation is also noted at pH 7 and 9. Although the present PCD trends as a function of the given experimental parameters look complicated and are difficult to be elucidated (Fig. 1 and Table 1), it is clear at a glance that the presence of fluoride affects not only the PCD rate but also the mechanistic paths of TMA degradation (i.e., the intermediate/product distribution).

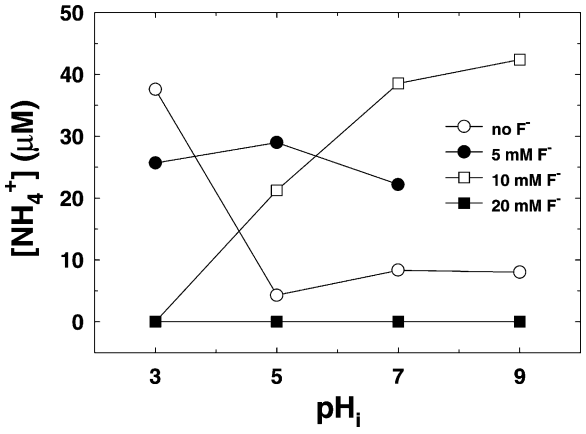

Fig. 2. Ammonium formation after 6 h PCD of TMA as a function of the initial pH and fluoride concentration. $[TMA]_0 = 100\,\mu M$, $[TiO_2] = 0.5$ g/l.

The aforementioned differences between the naked-TiO_2 and F–TiO_2 photoreactivities (Fig. 1 and Table 1) could be ascribed to the variations in the TiO_2 surface speciation and the related phenomena. The surface speciation modeling results were obtained by employing the diffuse layer model option in the MINTEQA2/PRODEFA2 software [20] and a surface site density of 2.5×10^{-4} mol/g that has been reported earlier for the Degussa P25 TiO_2 [21–23]. The following surface reactions were considered:

$$Ti\text{–}OH_2^+ \leftrightarrow Ti\text{–}OH + H^+ \quad (1)$$

$$Ti\text{–}OH \leftrightarrow Ti\text{–}O^- + H^+ \quad (2)$$

$$Ti\text{–}OH + H^+ + F^- \leftrightarrow Ti\text{–}F + H_2O \quad (3)$$

Reactions (1) and (2) are typically used to represent the naked-TiO_2 surface in contact with the aqueous media. For Degussa P25 TiO_2, surface acidity constant (pK_1 and pK_2) values of 3.9 and 8.7 have been reported for reactions (1) and (2), respectively [21–23]. As for the fluoride adsorption, a monodentate/anionic type of surface complex was assumed, as written in reaction (3). A pK_3 value of −7.8 has been reported for such a complexation [24]. The present model-estimated fluoride adsorption results, which were obtained using a pK_3 value of −8.2, also provide a good match with the experimental fluoride adsorption data as shown in Fig. 3. Hence the pK_3 value of −8.2 was used in this study. The fluoride concentration (i.e., 0.1 mM) used for the adsorption experiment is much lower than the actual fluoride concentrations employed in the PCD experiments (>5 mM) due to the analytical limitation in detecting small changes in fluoride concentrations ($\Delta[F^-]_{eq}$) resulting from adsorption.

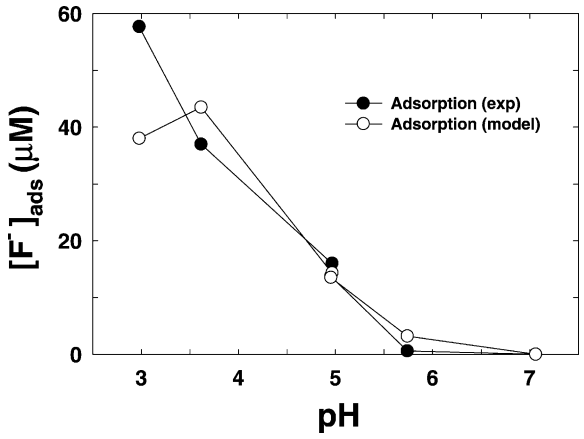

Fig. 3. Experimental and modeling results of F^- adsorption on TiO_2 as a function of pH. The modeling results were obtained using MINTEQA2 [20]. $[F^-] = 0.1$ mM, $[TiO_2] = 0.5$ g/l.

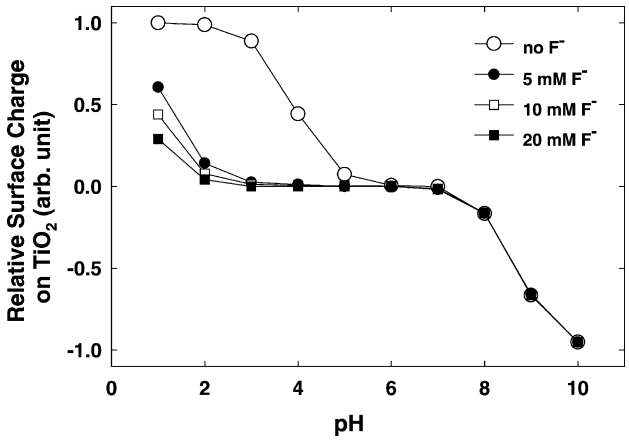

Fig. 4. Calculated surface charge on TiO_2 (on a relative scale) as a function of pH and $[F^-]$. Ti–OH_2^+ and Ti–O^- species contribute the positive and negative surface charge, respectively whereas Ti–OH and Ti–F species are taken as neutral.

Therefore, the pH-dependent F^- adsorption data in Fig. 3 should not be directly compared with the pH-dependent surface concentrations of Ti–F species that are calculated using higher $[F^-]$ (>5 mM) (see Table 2). TMA and Na^+ adsorption is not considered in the surface speciation modeling since their adsorption on both naked-TiO_2 and F–TiO_2 was found to be negligibly small.

The fluoride-induced modification in the surface speciation accompanies the change in the surface charge of TiO_2. Fig. 4 compares the calculated relative surface charge of naked-TiO_2 and F–TiO_2 as a function of pH and $[F^-]$. The positive surface charge of TiO_2 in the acidic pH region is markedly reduced with the addition of F^- because the dominant surface species shift from Ti–OH_2^+ to Ti–F. Therefore, the electrostatic interaction between the TMA cations and the TiO_2 surface should be affected not only by pH but also by the presence of fluoride. However, it should be noted that the surface charge of TiO_2 is not affected by the fluoride concentration in 5–20 mM range over the pH region of PCD experiments (pH 3–9).

TMA concentrations at the TiO_2/water and F–TiO_2/water interface regions were directly monitored by ATR-FTIR method. Fig. 5 compares the pH-dependent interfacial concentrations of TMA on naked-TiO_2 and F–TiO_2 films. The IR absorption peak at 1489 cm^{-1} is used for the quantification of TMA [7]. The interfacial concentration of TMA at pH 3 is higher on F–TiO_2 than naked-TiO_2 film whereas

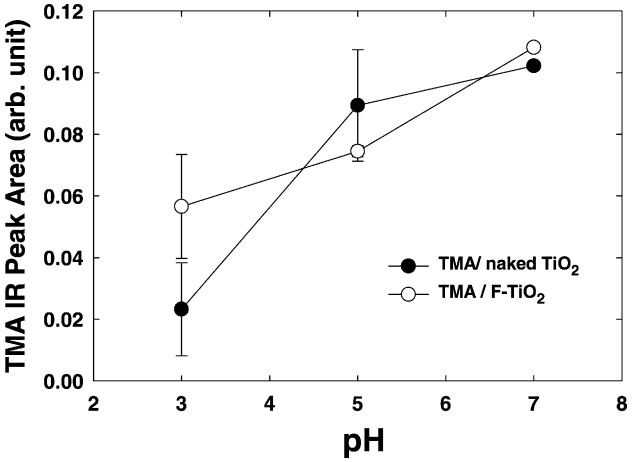

Fig. 5. Relative TMA concentrations (monitored by ATR-FTIR) at the surface/water interface of naked-TiO_2 and F–TiO_2 films as a function of pH. The ordinate scale is the integrated ATR-IR peak area of TMA. $[TMA] = 5$ mM, $[F^-] = 10$ mM.

little difference is noted at pH 5 and 7. This indicates that more TMA cations are attracted to the F–TiO_2 surface due to the reduced positive surface charge on F–TiO_2 (Fig. 4). At pH 5 and 7 where the surface charge is little affected by the presence of F^-, TMA interfacial concentrations are not

Table 2
TiO_2 surface species distribution (%) calculated using the MINTEQA2 software [20]

$[F^-]$ (mM)	pH 3				pH 5				pH 7				pH 9			
	0	5	10	20	0	5	10	20	0	5	10	20	0	5	10	20
[Ti–OH_2^+]	89	2.6	1.3	0.7	7.4	1.0	0.5	0.3	–	0.1	0.1	0.1	–	–	–	–
[Ti–OH]	11	0.3	0.2	0.1	92.6	12.3	6.7	3.2	98	91.4	85.3	77.2	33.4	33.4	33.4	33.4
[Ti–O^-]	–	–	–	–	–	–	–	–	2	1.8	1.7	1.5	66.6	66.6	66.6	66.6
[Ti–F]	–	97.1	98.5	99.2	–	86.7	92.8	96.5	–	6.7	12.9	21.2	–	–	–	–

much affected. An alternative explanation is that the presence of Ti–F species increases the hydrophobicity of TiO_2 surface and in turn helps to attract TMA (a hydrophobic cation) closer to the catalyst surface.

Table 2 lists the results of TiO_2 surface speciation modeling under different conditions. At pH 3, the fluoride addition shifts the dominant surface species from the Ti–OH_2^+ to Ti–F (to near completion). In the absence of fluoride the relative concentrations of 89% Ti–OH_2^+ and 11% Ti–OH species are estimated at pH 3 whereas 99.2% Ti–F and 0.7% Ti–OH_2^+ are predicted with 20 mM fluoride. Such a near complete displacement of the surface Ti–OH groups by Ti–F species should significantly reduce the formation of surface OH radicals, which are the dominant oxidant in the PCD of TMA [7], and consequently the PCD rate. Therefore, the reduced photoreactivity of F–TiO_2 at pH 3 (Fig. 1) should be attributed to the lack of surface Ti–OH groups and the reduced OH radical formation. A gradual decrease in photoreactivity with increasing $[F^-]$ at pH 3 also supports this explanation (Fig. 1). However, this does not seem to agree with the observation that the interfacial TMA concentration at pH 3 is higher on F–TiO_2 than naked-TiO_2 (Fig. 5). This implies that not the access of TMA to the surface but the OH radical generation is critical for achieving efficient degradation of TMA. This is also consistent with our previous claim [7] that the PCD of TMA at acidic conditions is initiated by free OH radicals in the solution bulk, not on the TiO_2 surface. This negative effect of F^- on the PCD of TMA is, on the other hand, in contradiction to a previous observation [16] that the PCD of phenol on TiO_2 was enhanced in the presence of F^- in the similar pH region. The difference between the two photocatalytic systems could be ascribed to the different main oxidant species involved at the water/TiO_2 interface. When the TiO_2 surface is covered by Ti–F species, the PCD process is dominantly initiated by the direct transfer of valence band (VB) holes [16] via which the phenol degradation on F–TiO_2 can proceed. However, the PCD of TMA that has a low probability of directly reacting with VB holes should be reduced on F–TiO_2.

At pH 5 where the surface coverage by Ti–F species is still dominant but not complete, a smaller fraction of surface Ti–OH groups do remain available for the OH radical formation. However, the surface speciation trend at pH 7 is largely different from that at pH 5 showing dominant Ti–OH and minor Ti–F species. Enhanced PCD of TMA is obtained under this condition (Fig. 1) as in the previous case of phenol degradation. According to Minero et al. [16,17], the preferential formation of free OH radicals on F–TiO_2 (reactions (4) and (5)) should be responsible for this fluoride-enhanced PCD:

$$h^+_{vb} + H_2O_{ad} \rightarrow H_2O^{\bullet +} \quad (\text{on F–TiO}_2) \tag{4}$$

$$H_2O^{\bullet +} \rightarrow H^+ + OH^{\bullet}_{free} \quad (\text{on F–TiO}_2) \tag{5}$$

$$h^+_{vb} + \text{Ti–OH}_{surf} \rightarrow \text{Ti–OH}^{\bullet +}_{surf} \quad (\text{on naked-TiO}_2) \tag{6}$$

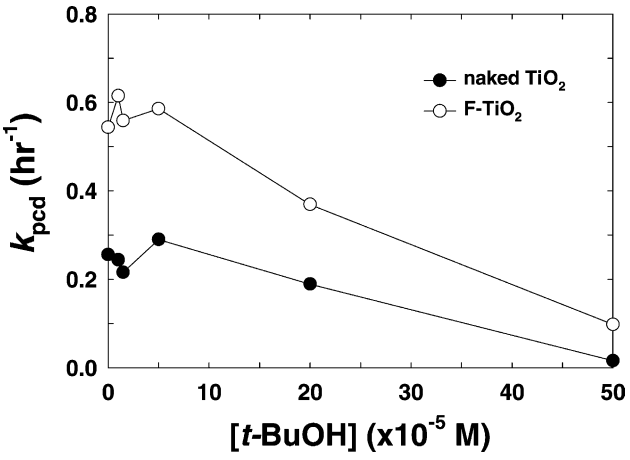

Fig. 6. Effect of *tert*-butyl alcohol (*t*-BuOH) concentration on the TMA PCD rate constant (k_{pcd}) in the suspensions of naked-TiO_2 and F–TiO_2. $[TMA]_0 = 100\ \mu M$, $[TiO_2] = 0.5$ g/l, $[F^-] = 10$ mM, $pH_i = 7$.

However, the role of free OH radicals does not explain the reduced PCD of TMA on F–TiO_2 at pH 3.

To verify the involvement of OH radicals in the naked-TiO_2 and F–TiO_2 systems, TMA PCD was also studied as a function of *tert*-butyl alcohol (*t*-BuOH, an OH radical scavenger) concentration, as shown in Fig. 6. Though the rate quenching by *t*-BuOH shows a similar trend in both systems, the photoreactivity of F–TiO_2 is consistently higher than that of naked-TiO_2. If the preferential formation of free OH radicals on F–TiO_2 is responsible for its higher reactivity, its photoreactivity enhancement over that of naked-TiO_2 should be absent in the presence of $[t\text{-BuOH}] > 5 \times 10^{-5}$ M because almost all the free OH radicals would be scavenged by the *t*-BuOH. For example, based on $k(t\text{-BuOH} + OH^{\bullet}) = 6 \times 10^8\ M^{-1}\ s^{-1}$, $k(TMA + OH^{\bullet}) = 7 \times 10^6\ M^{-1}\ s^{-1}$, $[t\text{-BuOH}] = 5 \times 10^{-5}$ M, and $[TMA] = 10^{-4}$ M, we estimate that 97.7% of free OH radicals should react with *t*-BuOH. Under this condition, the higher photocatalytic reactivity of F–TiO_2 should not be ascribed to the higher concentration of free OH radicals generated on F–TiO_2. In addition, it should be noted that the overall PCD of TMA involves not only OH radicals but also conduction band (CB) electrons whose transfer processes could also be affected by the fluorination of TiO_2 surface [7]. It has been reported that the band edge potentials shift upon the fluorination of TiO_2 [25,26]. This should alter the interfacial e^-/h^+ transfer kinetics on the TiO_2 particle.

The addition of fluoride at pH 9 shows no noticeable effect on the TiO_2 surface speciation (Table 2) and hence little changes the PCD rate of TMA (Fig. 1). Nevertheless, the product and intermediates distribution at pH 9 still exhibits a notable dependence on $[F^-]$ as shown in Table 1, which we do not have a clear explanation for. In particular, a drastic difference in NH_4^+ formation between the 10 and 20 mM fluoride systems (at pH 5–9) should be noted

(Fig. 2). Considering that both the surface concentration of Ti–F species and the surface charge are very similar between the cases of 10 and 20 mM fluoride added (Table 2 and Fig. 4), the fluoride effects on the product formation seem to result from some unknown homogeneous reaction mechanisms. A possible speculation could be an ion-pair formation between the F^- anions and TMA/intermediate cations that may have some impact on the PCD process.

4. Conclusions

The present study demonstrates that the PCD reactions of TMA are significantly influenced by the fluorination of TiO_2 surface and the consequent changes in the surface speciation. Not only the PCD rate but also the product/intermediates distribution is affected by the fluoride addition. A near complete transition from the $Ti–OH_2^+$ to Ti–F surface species at low pH markedly reduces the PCD rate because of the reduced OH radical formation. However, in the pH 5–7 region where sufficient surface OH groups do remain available along with the Ti–F species, the formation of surface OH radicals is allowed and the PCD rate of TMA is enhanced with the fluoride addition. Although the preferential formation of free OH radicals on $F–TiO_2$ has been previously suggested as a main cause of increased photoreactivity [16,17], this does not suffice to explain the present case of TMA degradation. Even in the presence of excess *t*-BuOH that should scavenge free OH radicals completely, $F–TiO_2$ shows a higher photoreactivity over naked-TiO_2. In addition, the product formation from TMA degradation is influenced by the presence of F^- even at pH 9 where the surface speciation of TiO_2 should not be altered by the fluoride addition. Though the main cause of the noted fluoride effect remains largely unclear at this stage, the fluoride-enhanced PCD for a variety of substrates that have been observed in this and previous studies is certainly useful for practical applications.

In summary, the effect of fluoride on the photocatalytic reactions could be related with how the surface fluorination of TiO_2 changes the processes of interfacial e^-/h^+ transfer, OH radical formation, surface charge distribution, and the substrate–surface interaction. The presence of F^- may affect the reaction mechanism in the homogeneous solution phase. Further studies are called for to clarify this issue.

Acknowledgements

This work was supported by KOSEF through the Center for Integrated Molecular Systems (CIMS) and partly by the Brain Korea 21 project.

References

[1] D.F. Ollis, H. Al-Ekabi (Eds.), Photocatalytic Purification and Treatment of Water and Air, Elsevier, Amsterdam, 1993.
[2] M.R. Hoffmann, S.T. Martin, W. Choi, D.W. Bahnemann, Chem. Rev. 95 (1995) 69.
[3] H. Lee, W. Choi, Environ. Sci. Technol. 36 (2002) 3872.
[4] W. Choi, J.Y. Ko, H. Park, J.S. Chung, Appl. Catal. B 31 (2001) 209.
[5] W. Choi, S.J. Hong, Y.-S. Chang, Y. Cho, Environ. Sci. Technol. 34 (2000) 4810.
[6] Y. Cho, W. Choi, J. Photochem. Photobiol. A 148 (2002) 129.
[7] S. Kim, W. Choi, Environ. Sci. Technol. 36 (2002) 2019.
[8] J. Zhao, H. Hidaka, A. Takamura, E. Pelizzetti, N. Serpone, Langmuir 9 (1993) 1646.
[9] P. Pichat, C. Guillard, C. Maillard, L. Amalric, J.-C. D'Oliveira, in: D.F. Ollis, H. Al-Ekabi (Eds.), Photocatalytic Purification and Treatment of Water and Air, Elsevier, Amsterdam, 1993, pp. 207–223.
[10] D.W. Bahnemann, D. Bockelmann, R. Goslich, Solar Energy Mater. 24 (1991) 564.
[11] C. Kormann, D.W. Bahnemann, M.R. Hoffmann, Environ. Sci. Technol. 25 (1991) 494.
[12] K.E. O'Shea, C. Cardona, J. Photochem. Photobiol. A 91 (1995) 67.
[13] J. Schwitzgebel, J.G. Ekerdt, F. Sunada, S.-E. Lindquist, A. Heller, J. Phys. Chem. B 101 (1997) 2621.
[14] C. Anderson, A.J. Bard, J. Phys. Chem. B 101 (1997) 2611.
[15] H. Tada, M. Yamamoto, S. Ito, Langmuir 15 (1999) 3699.
[16] C. Minero, G. Mariella, V. Maurino, E. Pelizzetti, Langmuir 16 (2000) 2632.
[17] C. Minero, G. Mariella, V. Maurino, D. Vione, E. Pelizzetti, Langmuir 16 (2000) 8964.
[18] M. Abdullah, G.K.-C. Low, R.W. Matthews, J. Phys. Chem. 94 (1990) 6820.
[19] M.S. Vohra, K. Tanaka, Environ. Sci. Technol. 35 (2001) 411.
[20] J.D. Allison, D.S. Brown, K.J. Novo-Gradac, MINTEQA2/PRODEFA2, A Geochemical Assessment Model for Environmental Systems, User's Manual, Version 3.0, US Environmental Protection Agency, Athens, Georgia, EPA/600/3-91/021, 1991.
[21] A. Torrents, A.T. Stone, Environ. Sci. Technol. 27 (1993) 1060.
[22] A.T. Stone, A. Torrents, J. Smolen, D. Vasudevan, J. Hadley, Environ. Sci. Technol. 27 (1993) 895.
[23] D. Vasudevan, A.T. Stone, Environ. Sci. Technol. 30 (1996) 1604.
[24] M. Herrmann, U. Kaluza, H.P. Bohem, Z. Anorg. Chem. 372 (1970) 308.
[25] C.M. Wang, T.E. Mallouk, J. Phys. Chem. 94 (1990) 4276.
[26] C. Lai, Y.I. Kim, C.M. Wang, T.E. Mallouk, J. Org. Chem. 58 (1993) 1393.